Tribology International 151 (2020) 106390

Contents lists available at ScienceDirect

Tribology International

journal homepage: http://www.elsevier.com/locate/triboint

# How lubricant formulations and properties influence the performance of rotorcraft transmissions under loss of lubrication conditions

Azhaarudeen Anifa Mohamed Faruck [a,b,*], Chia-Jui Hsu [a,b], Nicole Doerr [b], Michael Weigand [a], Carsten Gachot [a]

[a] TU Wien – Institut für Konstruktionswissenschaften und Produktentwicklung (IKP), Tribology Research Group, 1060, Vienna, Austria
[b] AC2T Research GmbH, Viktor-Kaplan-Straße 2C, Wiener Neustadt, Austria

ARTICLE INFO

*Keywords:*
Gears
Scuffing
Starved
Zinc dialkyldithiophosphate
Tricresylphosphate

ABSTRACT

Loss of lubrication (LOL) in a rotorcraft transmission causes erratic degradation of drivetrain components due to direct surface contact thereby increasing the frictional heat in the system. This article studies the ability of synthetic and mineral-based lubricating oils typically used in the aviation industry regarding their physical properties, chemical composition, and detailed chemical structure to extend the longevity of the rotorcraft transmissions in the event of LOL. The lubricating oils were subjected to boundary lubrication tests using a FZG gear test rig and two lab-scale tribometers, cylinder-on-ring and ball-on-disc. The results provide an enhanced ranking of the selected lubricating oils based on their load-carrying capacity and scuffing resistance under LOL conditions complemented by the consideration of the oil chemistry.

## 1. Introduction

Loss of lubrication (LOL) causes premature failure of gear and bearing components in a gearbox. Rotorcraft transmission systems that suffer from LOL are highly erratic due to high speed (20000 rpm) and high loading (1700 kW) contacts that amplify the failure rates tremendously until complete destruction of the rotorcraft. Several rotorcraft accidents have been caused by said LOL in the main gearbox including an accident of a Sikorsky (S-92) helicopter that took 17 human lives in April 2009 [1]. All aviation safety agencies around the globe demand that the LOL conditions will prevent continued safe flight for at least 30 min after perception of the low oil pressure by the flight crew [2,3]. Both, civil and military rotorcrafts require extensive testing of their drive train subsystems under LOL conditions in order to attain the airworthiness certification. Moreover, further operational and future rotorcraft developments impose even additional LOL time to enhance the operational safety limit.

Rotorcraft gears operate under higher speed, load and surface temperatures than most of the other gears (e.g. industrial gears, automotive gears). When a gearbox lubrication system fails under operation, several failures occur simultaneously, and they are accelerated by the temperature rise as there is no more sufficient heat transfer from the gear tooth surfaces by the lubricating oil. A combination of physical phenomena has been associated with the increase in surface temperature, which includes breakdown of the fluid film, desorption of boundary films, thermal or oxidative decomposition of the entrained lubricant, asperity heating and deformation [4]. It is known that the surface failures occur at some point under oil loss conditions when the lubricant film collapses at the gear tooth interface producing mainly scuffing as a sudden catastrophic failure. Conventionally, scuffing occurs when the fluid film thickness become less than the average height of the roughness peaks of the sliding surfaces, i.e. under boundary lubrication condition [5]. High sliding speed and prolonged frictional contact can change the metallic surface morphology (asperities) from its initial state, thereby, enduring transition from the boundary lubrication regime to scuffing wear [6,7]. According to Davis [8] the general mechanism for scuffing is caused by intense frictional heating generated by a combination of high sliding velocities and high contact stress conditions. Several theories were reported in relation with the initiation of scuffing: energetic activation of the rubbing surfaces [9,10], attaining critical temperature at the asperities [11–13], kinetics of oxide film formation [6,14], interaction between surfaces and the polar constituents of lubricants [15–17]. Despite numerous studies on scuffing failure analysis, a common

* Corresponding author. TU Wien – Institut für Konstruktionswissenschaften und Produktentwicklung (IKP), Tribology Research Group (E307-02-3), Getreidemarkt 9, 1060, Vienna, Austria.
*E-mail addresses:* azhaarudeen.faruck@tuwien.ac.at, azhaarudeen.faruck@ac2t.at (A.A. Mohamed Faruck), chia-jui.hsu@tuwien.ac.at, Chia-Jui.Hsu@ac2t.at (C.-J. Hsu), nicole.doerr@ac2t.at (N. Doerr), michael.weigand@tuwien.ac.at (M. Weigand), carsten.gachot@tuwien.ac.at (C. Gachot).

https://doi.org/10.1016/j.triboint.2020.106390
Received 5 March 2020; Received in revised form 20 April 2020; Accepted 22 April 2020
Available online 11 May 2020

**Abbreviation**

| | |
|---|---|
| $F_N$ | Normal force. N |
| Fr | Friction force. N |
| a | major axis of an elliptical wear scar. mm |
| b | minor axis of an elliptical wear scar. mm |
| B | Brugger load-carrying capacity. N/mm$^2$ |
| $h_{min}$ | minimum fluid film thickness. nm |
| σ | Composite roughness. μm |
| $Ra_1$ | average roughness of surface 1. μm |
| $Ra_2$ | average roughness of surface 2. μm |
| λ | Lambda ratio. |
| LOL | Loss of lubrication |
| FZG | Forschungsstelle für Zahnräder und Getriebebau |
| FTIR | Fourier-transform infrared spectroscopy |
| ICP-OES | Inductively coupled plasma optical emission spectrometry |
| GC-FID | Gas chromatography coupled with flame ionization detection |
| MS | Mass spectrometry |
| ATR | Attenuated total reflection |
| PAO | Polyalphaolefin |
| ZDDP | Zinc dialkyldithiophosphate |
| TCP | Tricresyl phosphate |
| BuTPP | Butylated triphenyl phosphate |

identification mechanism for the prediction of scuffing initiation is still undefined.

On the other hand, gear failures are strongly influenced by the base oil properties such as viscosity, viscosity-index, viscosity-pressure behavior and the type of additives used [18–20]. Given the fact that the LOL condition eliminates the effect of viscosity of the lubricating oil, the load bearing capacity is only given by the boundary films formed before and during oil loss. The additive elements that produce exceptionally durable boundary layers are of interest, consequently, investigating lubricating oils from different groups with different blends of additive elements may shed more light onto the underlying mechanisms. J. M. Martin et al. [21–23] investigated several tribofilms to evaluate their friction responses and wear protection mechanisms using innovative test approaches.

Aviation oils are designed to operate at higher temperatures (200 °C); therefore, oils with excellent thermal stability and good tribological properties can provide enough lubrication of metal surfaces to reduce friction and prevent wear. Synthetic base stocks such as esters containing phosphate esters form short chain polyphosphate glasses protecting the bearing metal surfaces [24]. Earlier studies on rotorcraft gearbox lubrication were conducted using lubricating oils containing extreme pressure additives mainly to improve the load-carrying capacities, scuffing and pitting failures [25]. Therefore, the main objective of this work is to experimentally find the effects of lubricating oil properties and their detailed chemistry on the gear scuffing failure under oil starvation conditions.

Gear lubrication studies are often conducted only in gear test rigs using specified gear geometries and standardized test conditions. For example, the standard FZG back-to-back gear test rig (FZG) that has been developed over many years as well as improved for simulating different types of gear failures [26,27]. Typical gear failure modes under lubrication such as scuffing (A/8.3/90), micro-pitting (GF-C/8.3/90) and pitting (PT-C/9:10/90) performances are determined using FZG gear test rig. However, test methods representing the conditions of LOL for high-speed rotorcraft transmission components are not feasible. System level attempts were made in the past both experimentally and theoretically to understand the LOL behavior in rotorcraft transmission drive trains [25,28,29]. Gasparini et al. [30] implemented design changes and applied alternative materials, surface finishes and coatings that lasted 50 min after LOL in the recent civil certification test for Augusta Westland (AW189) transmissions. Although, full-scale studies often generate high costs and produce lots of information deviating from the focus of the research. Alternatively, the standard FZG gear test rig is originally not designed to perform tests under oil loss conditions but can be modified. Nevertheless, other tribometrical methods that can simulate a single point of the contact of a gear mesh such as ball-on-disc and twin discs can be used to investigate oil loss or LOL behavior as well. Riggs et al. [31] established LOL experiment protocols using a high-speed ball-on-disc tribometer measuring the relative time to scuffing initiation for different combinations of lubricant, material and surface finish indicating that varying the properties of contacting materials and lubricating oil formulations could improve the survivability of the aircraft in the event of LOL. Few recent studies utilized lab-scale methods to focus on low-friction coatings and lubricant modifications for operation during LOL conditions [32–34]. Yet, specific in-depth research on lubricating oil chemistry that influence the performance of the rotorcraft transmission components under LOL condition is rarely found. The time between the start of LOL and initiation of scuffing is crucial and it depends on the effectiveness of lubricant interaction with the surfaces. This work attempts to find the significance of the lubricating oil properties and additive chemistry in order to improve the survivability of rotorcraft transmission components in the event of LOL.

The influence of quite different groups of oils with dissimilar viscosities on gear performance and the effect of wear-protective additives under LOL conditions are evaluated. Five rotorcraft lubricating oils that are aviation approved and used were chosen for this study. Besides conventional lubricant analysis such as Fourier-transform infrared spectroscopy (FTIR) and inductively coupled plasma optical emission spectrometry (ICP-OES), advanced lubricant analysis by gas chromatography coupled with flame ionization detection (GC-FID) and high-resolution mass spectrometry (MS) were also applied to allow for further insights into the chemistry of the base oils and wear-protective additives. The gear tests were carried out using a FZG back-to-back gear test rig under (dip) lubrication. The LOL experiments were conducted by two lab-scale, i.e. cylinder-on-ring and ball-on-disc, tribometers. On the one hand, experiments in lubricated mode reveal the scuffing, micro-pitting and pitting failures of gears. On the other hand, LOL experiments focus on the load-carrying capacity and friction behavior of the selected lubricating oils under oil starvation conditions.

## 2. Materials and methods

### 2.1. Lubricant selection and characterization

In this work, three ester-based synthetic lubricating oils, one polyalphaolefin (PAO) mixed with traces of ester synthetic lubricating oil and one mineral based lubricating oil, all containing different additive packages were evaluated for their performance in both lubricated and starved condition for their application in rotorcraft transmission. The lubricating oils were named as three turbine oils (Oils A, B and C), one automatic transmission fluid (Oil D) and one piston engine oil (Oil E).

#### 2.1.1. Conventional analytical methods

The kinematic viscosities of these oils were analyzed using a Stabinger viscometer SVM 3000 (Anton Paar, Graz, Austria) according to ASTM D 7042 [35] at both 40 °C and 100 °C. The corresponding viscosity indices were calculated according to ASTM D 2270 [36]. The elemental contents were determined with ICP-OES (iCAP 7400 ICP-OES Duo, Thermo Fisher, Waltham, MA, USA) after microwave treatment with nitric acid. Quantification was based on aqueous calibration

standards. FTIR measurements were performed by using a Bruker Tensor 27 (Brucker, Ettlingen, Germany) equipped with an attenuated total reflection (ATR) unit. The instrument was configured to cover the mid-infrared range of 4000 $cm^{-1}$ to 500 $cm^{-1}$ and a resolution of 4 $cm^{-1}$.

#### 2.1.2. Advanced analytical methods

In order to gain more knowledge of oil compositions, not so common analytical methods were added to the conventional ones mentioned in previous section. In detail, GC-FID was used to determine the boiling point distribution as an estimate of the ability to remain on hot surfaces, e.g., initiated by higher friction. As second advanced analytical method, high-resolution MS enabled the identification of the main base oil and wear-protecting additives. Both MS and GC-FID helped to determine the base oil groups, the knowledge of which was crucial for determining the pressure-viscosity coefficients. Base oil chemistries were analyzed using a Trace GC Ultra equipped with a FID (Thermo Fisher Scientific, Austin TX, USA) comprising an autosampler (TriPlus Autosampler, Austin TX, USA). For the determination of the boiling point distribution, a simulated distillation based on ASTM D6352 [37] was done. The method covered a boiling range of petroleum distillate fractions from an initial boiling point greater than 174 °C (345 °F) and a final boiling point of less than 700 °C (1292 °F) for C10 to C90 alkanes referred to atmospheric pressure. A sample aliquot was diluted to 4% with n-heptane and introduced into the chromatographic system. For separation, a non-polar GC column (TraceGOLD TG-1MS, 100% dimethyl polysiloxane, 15 m length, 0.25 mm inner diameter, 0.25 μm film thickness) was purchased from Thermo Scientific (Waltham, MA, USA). At a constant gas flow of 10 mL/min helium, the oven containing the GC column was heated from initially 50–300 °C at a heating rate of 10 °C/min and then held at 300 °C for 30 min. The eluted compounds were detected by FID. The obtained chromatograms were analyzed according to ASTM D6352 with Thermo Xcalibur v2.0 software (Austin, TX, USA) to obtain the boiling point distributions, i.e., simulated distillation curves. For better comparability, the simulated distillation curves of the oils are presented together with the boiling points of a standard mixture composed of C10 to C40 alkanes.

High-resolution MS was used to characterize the base oils and wear-protective additives in the five selected lubricants based on methods successfully applied to engine oils [38–40]. The oil samples were dissolved in a methanol-chloroform mixture (v:v 3:7, dilution factor of 1000) and then subjected to a LTQ Orbitrap XL hybrid tandem mass spectrometer (ThermoFisher Scientific, Bremen, Germany) by direct infusion at a flow rate 5 μL/min. Ionization of the analytes (sample molecules) was achieved by electrospray ionization (ESI) with the following parameters: Spray capillary temperature of 275 °C, spray voltage of 4.0 kV, capillary voltage of −35 V for negative and +39 V for positive ion mode. Nitrogen was used as sheath gas, and helium as buffer gas. The generated ions were accelerated under an electrical potential to increase the kinetic energy allowing them to collide with helium gas. Low-energy collision-induced dissociation (CID) was performed for the elucidation of chemical structures with a normalized collision energy optimized between 20 and 40%. CID generated ion products were produced in a linear ion trap device and detected by the high-resolution orbitrap-section of the instrument at a resolution of 60,000 (full width at half maximum, FWHM). The software tools Xcalibur version 2.0.7 and Mass Frontier version 6.0 (both ThermoFisher Scientific, Bremen, Germany) were applied for data evaluation. All mass measurements were acquired with a mass accuracy of 5 ppm or better.

### 2.2. Tribometrical experiments

#### 2.2.1. FZG back-to-back gear test rig

Oil viscosity, type of base oil and additive composition play a significant role in gear failure modes. Typical gear failures such as scuffing, micro-pitting and pitting are strongly influenced by the lubricants and their properties. FZG back-to-back gear test rig (Technische Universität München, Garching, Germany) is a standard gear failure simulation test method according to ISO 14635 [41] developed continuously over many years for lubricant investigations used in industrial and automotive gearboxes. Mainly two types of gear geometries are used to evaluate gear failures, type A for scuffing load capacity and type C for wear, micro-pitting, and pitting failures. In scuffing tests, the gears are loaded in 12 increasing load steps from lower to higher Hertzian stresses each tested for 15 min and the test begins once the oil temperature reaches 90 °C. After each load stage, the gear flanks are inspected visually for scuffing marks and the gears are weighed to determine their weight loss. When cumulative scuffing marks observed from all teeth of the pinion exceed the width of one tooth then the critical load stage is achieved. The test parameters and the evaluation of micro-pitting and pitting results based on the standard test methods are described in Ref. [27]. The FZG back-to-back test gear rig consists of two test gears and two slave gears as shown in Fig. 1. The test gears have a center distance of 91.5 mm and are connected to the respective slave gears by two shafts. A load clutch is in place on one of the shafts that allows the shaft to fix the half of the shaft to the base with the locking pin and the other half is twisted to apply the desired torque load, e.g., by means of a lever and weights. Thus, a static torque is applied between the test gears and the load used to apply the torque is removed after securing the clutch together. The test gears are splash lubricated, and the lubricant temperature is monitored using a temperature controlling unit. In this work, separate gear pairs (pinion and wheel) are used for individual gear failure modes (scuffing, micro-pitting and pitting) and each lubricating oil was tested twice using the two faces of the gear pairs. Since, Oil A and B are successive generations belonging to the same lubricating oil type, the scuffing test was carried using only one gear pair. Though, FZG back-to-back test gear rig provides results close to the application under lubrication, the LOL condition experiments were done by using lab-scale tribometer bench tests to study the influence of lubricant chemistry.

#### 2.2.2. Brugger lubricant tester

The determination of load-carrying capacity of lubricating oils was carried out using a Brugger lubricant tester according to the standard DIN 51347 [42] under room temperature and pure sliding conditions. The Brugger test enables the lubricants to form a thin layer in the cylinder-on-ring contacts operating under boundary lubrication regime. The lubricating oil is poured on a rotating ring ensuring the oil spreads over the complete surface and a stationary cylinder is pressed from the top on the ring surface with a constant applied load. The cylinder and the ring are fixed at right angles to each other. The test produces an elliptical wear scar with the lengths a and b in X and Y direction are shown in Fig. 2. Using the normal load $F_N$ and the lengths a and b as shown in Eq. (1), the Brugger load-carrying capacity B of each lubricant is calculated. Brugger experiments were repeated five times for each lubricating oil under same test conditions.

$$B = \frac{4^{*}F_N}{a^{*}b^{*}\pi}\left(\mathrm{N/mm^2}\right) \quad \text{Eq.1}$$

#### 2.2.3. Schwing-Reib-Verschleiß (SRV) tribometer

Friction measurements were carried out using a Schwing-Reib-Verschleiß (SRV) tribometer (Optimol Instruments Prüftechnik GmbH, Munich, Germany) under pure sliding conditions. A stationary ball is pressed against a rotating disc with a fixed track radius at a constant speed and a point load; test specimens and the lubricants are heated to 100 °C. The experimental parameters and conditions are summarized in Table 1. The friction experiments were conducted mainly in three stages starting with 10 min running-in stage with lubricant supply, followed by 30 min of the main stage without lubricant supply where the oil supply was shut-off and finally the experiment is continued for additional 10 min. One of the main observations from friction measurements is the initiation of scuffing indicated by a sharp rise in the coefficient of

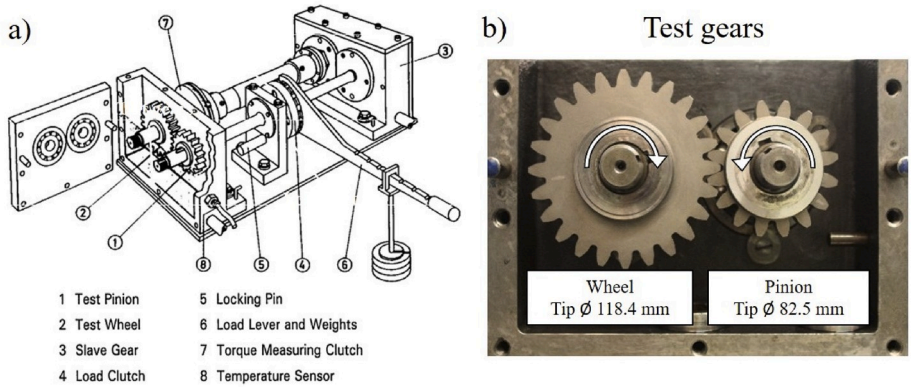


**Fig. 1.** Lubricant performances against scuffing, micro-pitting and pitting damages were evaluated on a) FZG back-to-back gear test rig [27] and b) shows a pair of test spur gears mounted on the rig, which are rotated against each other.

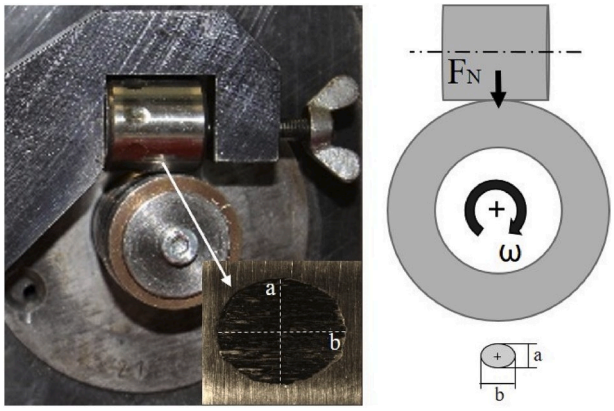


**Fig. 2.** Brugger tribometer showing the contact geometry and an elliptical wear scar in the insert indicating diagonal lengths a and b (left) and a schematic representation of the contact configuration (right).

**Table 1**
Parameters for the Brugger tests and SRV experiments.

| Parameters | Brugger - tribometer | SRV - tribometer |
|---|---|---|
| Material | Ring: X210CrW12<br>Cylinder: 100Cr6 | Ball and Disc: 100Cr6 |
| Dimention | Ring: Dia - 25 mm; W - 12 mm<br>Cylinder: Dia - 18 mm; W - 18 mm | Ball: Dia - 10 mm<br>Disc: Dia - 100 mm; W - 10 mm |
| Hardness | 60 HRC | 60 HRC |
| Surface roughness (Ra) | Cylinder - 0.5 to 0.7 μm | Ball - 0.1 μm<br>Disc - 0.3 μm |
| Load | 400 N | 1.5 GPa (maximum Hertzian pressure) |
| Speed | 900 rpm | 5 m/s |
| Test duration | 30 s | 10 min: Running-in;<br>30 min: Loss of lubrication condition;<br>10 min: Additional loss of lubrication condition |
| Temperature | Room temperature | 100 °C +/- 5 °C |

friction mainly during the main stage without lubricating oil supply. The time between the oil supply shut-off and the scuffing initiation has been recorded as the time to failure or degradation of the tribofilm under LOL condition. Lubricants were constantly delivered in front of the contact throughout the running-in stage and each lubricating oil experiment was repeated 3 times. The setup of the SRV tribometer is shown in Fig. 3.

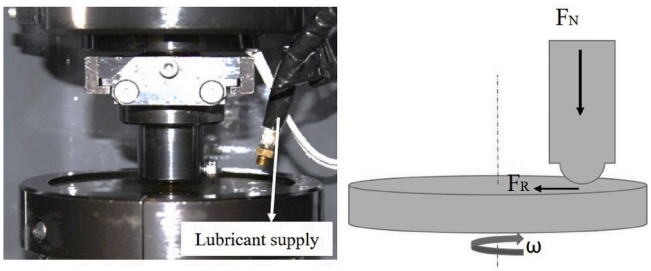


**Fig. 3.** SRV tribometer with view at the ball-on-disc set-up (left) and a schematic representation of the contact configuration (right).

### 2.3. Surface analysis

After every tribo-experiment using the five lubricating oils, the specimens were cleaned with toluene and petroleum ether using an ultrasonic bath to remove residual oil from the surface. The used specimens were then examined with different surface characterization methods as given below:

- Elliptical wear scars from Brugger cylindrical specimens were analyzed regarding the wear volume using a confocal and interferometric microscope (Leica DCM 3D, Leica Microsystems, Wetzlar, Germany).
- Wear tracks from SRV experiments were examined concerning the formation of tribofilm and its compositions using a scanning electron microscope (JSM-IT100, Freising, Germany) equipped with an energy-dispersive X-ray spectrometer (SEM-EDX) and Raman spectroscopy (HR800, Jobin Yvon Horiba, Darmstadt, Germany).
- Microstructural characterization of the selected wear tracks from SRV experiment was performed on thin lamellae prepared by focused ion beam (Dual Beam FIB FEI Quanta 200 3D). The electron transparent lamella samples were studied by transmission electron microscopy (TEM) using a FEI TECNAI F20 field emission TEM operated at 200 kV and equipped with a high brightness X-FEG cathode.
- Micro-pitting gear failures were analyzed using a digital microscope (VHX-6000 series, Keyence, Mechelen, Belgium).

## 3. Results

### 3.1. Conventional oil analysis

#### 3.1.1. Physical properties and chemical compositions

The oil specifications together with the physical and chemical

properties of the lubricants are presented in Table 2. Oils A and B are successive generations of aircraft gas turbine oils where Oil B exerts an improved thermal and oxidation stability in comparison with Oil A.

Oil C is approved for helicopter transmissions for operation at high temperature and high loads. As shown in Table 2, Oils A to C have similar viscosities and are equipped with phosphorus-containing additives to provide wear protection and load-carrying capacity. It is noted that the phosphorus content is 2.5 times lower for Oil C. Other elements were found only in negligible amounts.

Oil D is an automatic transmission fluid approved for aviation gearbox applications. The viscosity is slightly higher than for Oils A to C. Elemental analysis suggests additives with phosphorus and sulfur for wear protection. Calcium points to the use of a detergent, therefore, sulfur could be also found in sulfonate-based detergents.

Oil E is used in aviation piston engines. It is characterized by the highest viscosity of all oils within this study. Furthermore, higher levels of additive elements were identified, which are typical for engine oils. Phosphorus, sulfur and zinc constitute zinc dialkyl dithiophosphate (ZDDP) as typical anti-wear additive. Calcium can be found in detergents. The high content indicates the presence of calcium carbonate used as base reserve. The high sulfur content also suggests sulfonates as detergent but requires verification by other means.

### 3.1.2. FTIR analysis

FTIR complemented conventional analyses by molecular information about base oil and additive chemistry. Fig. 4 compares the infrared spectra of all five oils. The region from 3000 to 2800 $cm^{-1}$ is typical for hydrocarbon (C–H) bonds. It is unspecific as such peak can be found in every oil. As to Oils A to C, the spectra are widely identical and dominated by the carbonyl (C═O) bond at a wavenumber of 1740 $cm^{-1}$ and the C–O bond at about 1150 $cm^{-1}$. This points to an ester base oil, specifically a synthetic ester base oil to account for the thermal and oxidative stability needed in a helicopter transmission. The carbonyl peak area of Oil D is about 7% of that of Oil A. Thus, it can be concluded that Oil D also contains an ester base oil but only as a minor component in a hydrocarbon base oil. Oil E does not contain an ester component and hence the only base oil is a hydrocarbon. The fingerprint region that is below 1500 $cm^{-1}$ contains also valuable information about the wear-protective additives. Here, small peaks at a wavenumber of about 1000 $cm^{-1}$ indicate P–O bonds that can be identified in organic phosphates (Oils A to D) and ZDDP (Oil E). Furthermore, FTIR spectra indicate sulfonates as detergents in Oils D and E.

**Table 2**
Properties and chemical compositions of the lubricants selected.

| Lubricants | | Oil A | Oil B | Oil C | Oil D | Oil E |
|---|---|---|---|---|---|---|
| Specifications | | MIL-PRF 23699 | MIL-PRF 23699 | DOD-PRF-85734A | SAE-70W-80 | SAE-10W-40 |
| Physical properties | Unit | | | | | |
| Density @ 15 °C | g/cm$^3$ | 1.00 | 1.00 | 0.99 | 0.83 | 0.86 |
| Kinematic viscosity @ 40 °C | cSt | 25.4 | 27.8 | 26.8 | 39.3 | 93.8 |
| Kinematic viscosity @ 100 °C | cSt | 4.96 | 5.36 | 5.27 | 7.68 | 14.5 |
| Viscosity index | (–) | 122 | 130 | 132 | 170 | 159 |
| Chemical composition | | | | | | |
| Phosphorus (P) | ppm | 2400 | 2400 | 900 | 340 | 1000 |
| Sulfur (S) | ppm | <10 | <10 | <10 | 800 | 4600 |
| Zinc (Zn) | ppm | – | – | – | <10 | 1200 |
| Calcium (Ca) | ppm | <5 | <5 | <5 | 50 | 3300 |
| Silicon (Si) | ppm | <10 | <5 | <10 | <5 | <5 |

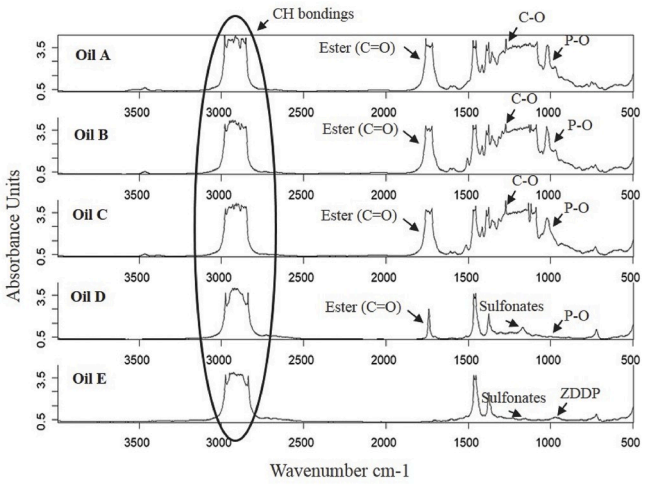


**Fig. 4.** ATR FTIR spectra of Oil A to E.

## 3.2. Advanced analytical methods

### 3.2.1. Boiling range distribution by simulated distillation

The chromatograms of Oils A to E are depicted in Fig. 5 together with alkane standards ranging from C10 to C40. All oils have specific patterns that allow for a further characterization of base oil chemistries. Oils A and B provide similar chromatograms thus suggesting that the same ester base stock is used. The main boiling range covers C26 to C40 referred to the alkane standard. In contrast to Oils A and B, GC-FID revealed a regular base oil pattern for Oil C where the individual peaks in the homologous series differ by one carbon atom. The compounds range from C27 to C40 when compared to the alkane standard. Two of the three main peaks of Oil D can be attributed to a poly-alphaolefin (PAO4 quality) with its peaks at 18.02 min and 22.79 min. The peak at 20.48 min refers to the ester base oil as already identified by FTIR. The ester base oil covers about 9% of the entire base oil peak area, thus confirming the estimate of 7% made by FTIR. Base oil molecules are distributed from C25 to C42. Eventually, Oil E shows a broad peak ranging from C20 to C42, which is typical for mineral oils.

The boiling point distributions of the five oils calculated from simulated distillations are illustrated in Fig. 6. Oil E shows the broadest boiling range and the lowest initial boiling point (IBP) of 342 °C, which points to higher volatility compared to the other oils. Oil D is characterized by a higher IBP of 380 °C, but about 70% of the base oil may evaporate below 430 °C. In contrast, the most important individual compounds in Oils A to C do not boil before 430 °C, the main boiling ranges stretch from about 430 to 500 °C with a slight advantage of Oil C (IPB of 431 °C) over Oils A and B (IBP of 363 and 411 °C). If a comparison is made regarding evaporation tendency, which is important with a view to availability at higher operating temperatures, the following ranking is given from highest to lowest IBP:

Oil C > Oil B > Oil D > Oil A > Oil E

### 3.2.2. Base oil and wear-protective additive chemistry by high-resolution MS

For the overall evaluation of the tribological performance of the five lubricating oils including the oil composition (see chapter 4), the findings from conventional and advanced analyses were combined and summarized in Table 3. The base oils of Oils A, B and C are synthetic ester base stocks composed of pentaerythritol as alcohol and mid-chain fatty acids ranging from C5 to C9. As the ester pattern of Oil C is different from these of Oil A and B (see Fig. 5), it is concluded that a different, most probably branched, fatty acid feed stock is used for Oil A and B. Oil

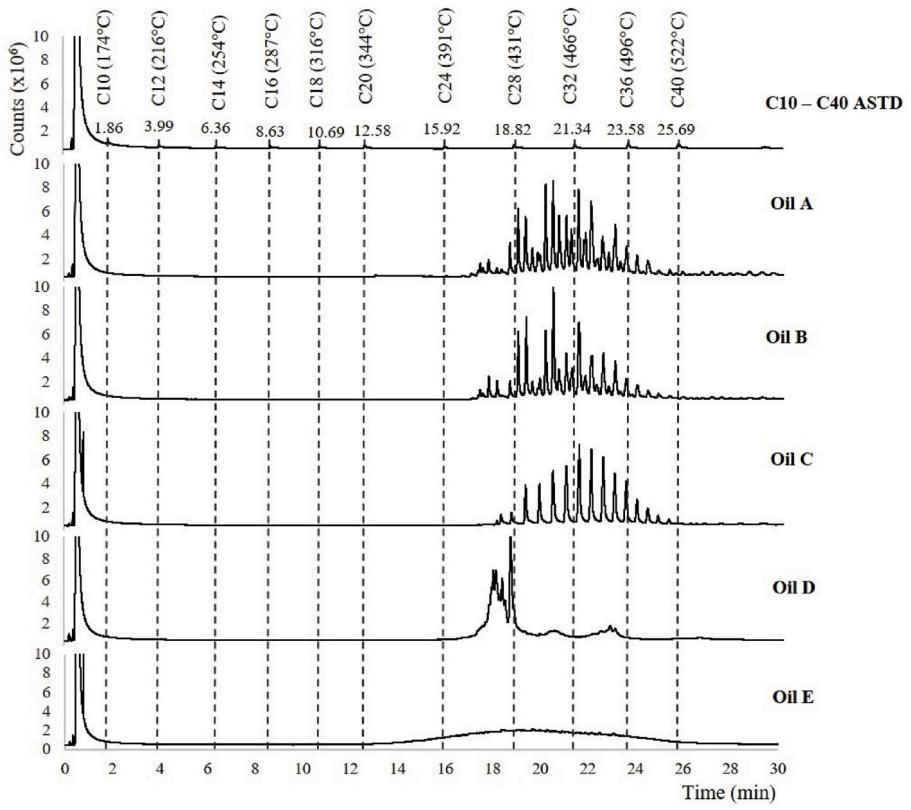


**Fig. 5.** GC-FID chromatograms of Oils A to E and C10 to C40 alkane standards, temperatures in brackets are the respective boiling points.

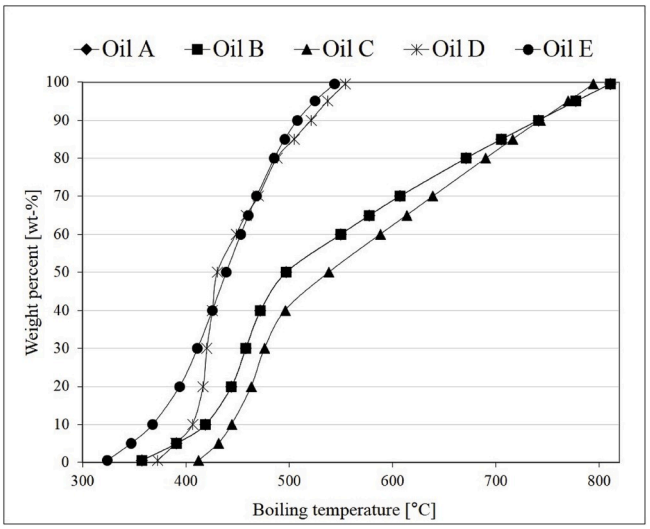


**Fig. 6.** Boiling point distribution of Oils A to E. The curves of Oils A and B are identical.

D is also made of fully synthetic base oils composed of PAO4 as main base oil and an ester as minor base oil component synthesized from a branched nonanedioic acid and decanol. Oil E is formulated from a mineral oil, group II or III, thus does not contain ester base oil. As to wear protection, MS analysis has shown that aromatic phosphates are used in four of the five oils. Oil A and C use tricresyl phosphate (TCP). Oil D contains butylated triphenyl phosphate (BuTPP). Oil B is equipped with a mixture of tricresyl phosphate and butylated triphenyl phosphate (BuTPP). As expected, Oil E as engine oil follows another strategy based on a zinc dibutyl dithiophosphate as major ZDDP compound.

From the above analytics (i.e. base oil type) of the lubricating oils, we could estimate the pressure-viscosity coefficient based on the empirical correlation by So and Klaus [43] and the minimum film thickness using Hamrock-Dowson equation [44]. Prior to the friction experiments pressure-viscosity coefficient, minimum fluid film thickness and lambda ratio (λ) for the given SRV experimental parameters were determined to verify whether the friction evaluation for all the lubricants was conducted under boundary lubrication (i.e. $\lambda < 1$), see Table 4. Lambda ratio is calculated by dividing the minimum film thickness ($h_{min}$) by the composite surface roughness (σ). The composite surface roughness of contacting surfaces (1 and 2) can be determined by taking the square root of the sum of the squares of average roughness values ($Ra_1$ and $Ra_2$) for each surface.

### 3.3. Scuffing, micro-pitting and pitting behavior evaluated by FZG test method

The relative ranking of the lubricating oils with respect to the scuffing failure is shown in Fig. 7. The scuffing test results represent the load-carrying capacities in terms of load levels to a maximum of 12; lubricating oil tests passing this maximum load level were qualified as high anti-scuffing performance oil under FZG back-to-back gear test rig conditions.

According to Fig. 7, Oils A and B have shown scuffing failures at load level 9 and 10, respectively, versus the maximum scuffing load level of 12. On the other hand, Oils C and Oil E had resisted the contacts without any significant scuffing failure thus showing that these lubricants could perform even beyond the load level 12. In case of Oil D, the scuffing load limit was reached at the load level 12 showing intermediate load-carrying capacity results relative to the other oils examined. Despite the pronounced difference in the kinematic viscosity of Oils C and E, their scuffing results are similar. Therefore, the ability of a lubricant to prevent scuffing under the given sliding conditions mainly depends on providing either enough fluid film lubrication or surface-binding

**Table 3**
Base oil and wear-protecting additive chemistries of Oils A to E. Exact positions of methyl and butyl groups in organic phosphates cannot be determined with MS, therefore other distribution than shown is possible.

| Lubricant | Base oil | Wear-protective additives |
|---|---|---|
| **Oil A** | Pentaerythrityl tetraalkanoic acid ester (exemplary structure, C5 to C9 fatty acids) 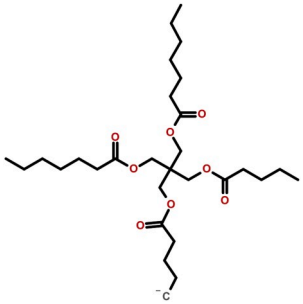 | Tricresyl phosphate 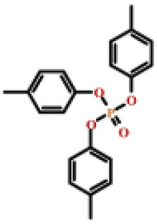 |
| **Oil B** | Pentaerythrityl tetraalkanoic acid ester (exemplary structure, C5 to C9 fatty acids) 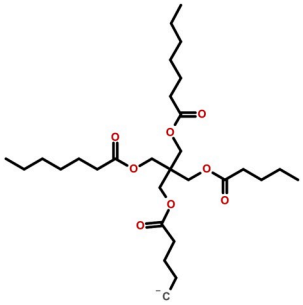 | Tricresyl phosphate and butylated phenyl phosphate 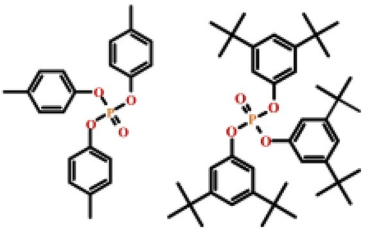 |
| **Oil C** | Pentaerythrityl tetraalkanoic acid ester (exemplary structure, C5 to C9 fatty acids) 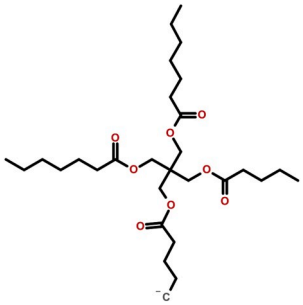 | Tricresyl phosphate 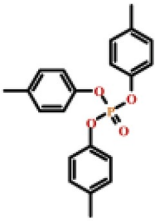 |
| **Oil D** | PAO 4 as main base oil<br>Didecyl nonanedioic acid ester 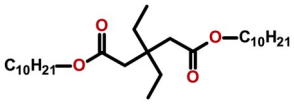 | Butylated phenyl phosphate 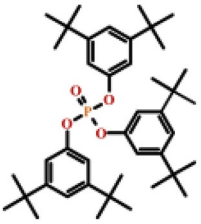 |
| **Oil E** | Hydrocarbon base oil (group II or III) | Zinc dibutyl dithiophosphate as main compound 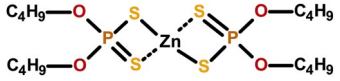 |

**Table 4**
Base oil types and corresponding calculated pressure-viscosity values and lambda ratios for the lubricating oils at 100 °C.

| Lubricating Oils | Base oil types | Pressure-viscosity coefficient (x10$^{-8}$ Pa$^{-1}$) | Minimum film thickness (nm) | Lambda ratio (−) |
|---|---|---|---|---|
| Oil A | Ester | 1.21 | 18.79 | 0.35 |
| Oil B | Ester | 1.20 | 19.67 | 0.37 |
| Oil C | Ester | 1.21 | 19.42 | 0.36 |
| Oil D | PAO + Ester | 1.25 | 22.75 | 0.42 |
| Oil E | Mineral | 1.40 | 37.80 | 0.70 |

additive compounds that continue to bear the load and therefore separating the surfaces.

In Fig. 8a, the micro-pitting results are shown as only visual aids to compare the difference in the surface profile modification and/or deviation. Micro-pitting failures are formed by large number of micro-cracks mainly at the dedendum part of the gear flank due to cyclic loading of the gears. These micro-cracks can in later stage lead to involute profile deviations in gear tooth geometry by loss of material, as well as influence the occurrence of pitting failures. The grey regions (micro-pitting) across the gear flanks in Fig. 8a were more evident for turbine oils (Oils A to C) than the automatic transmission fluid (Oil D) and engine oil (Oil E). The effect of lubricating oil properties and

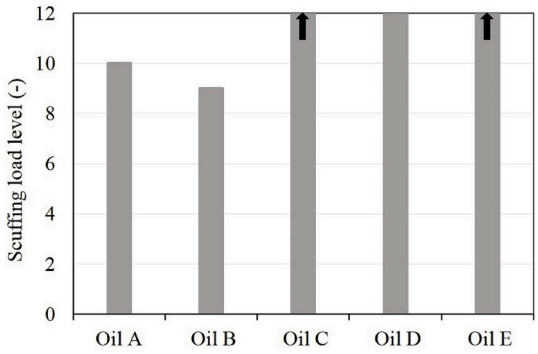


**Fig. 7.** FZG scuffing test results showing load-carrying capacities of the studied lubricating oils in terms of load levels and the arrows for Oils C and E indicating scuffing load capacities beyond load level 12.

additive composition were comparable only with the qualitative micro-pitting results. The micro-pitting failures produced in this work were correlating more with the lubricant viscosity than their chemical composition and so require base oil investigations to elaborate more. This is important to know as low viscosity grade oils with anti-wear and extreme pressure additive packages are preferred in most gearbox applications to prevent churning losses and to produce high torque efficiency. However, such measure increases the vulnerability of the machine elements thus contributing to additional risks under oil starvation conditions.

Pitting performances of the lubricating oils are represented in Fig. 8b as test hours until the occurrence of first pitting failure. The pitting results of the turbine oils were completely different from their scuffing load-capacity and micro-pitting behaviors. Oil B with low load-carrying capacity and micro-pitting performances has shown better pitting performance by operating about 235 h compared with Oil A and Oil C where their operating hours are even less than half of that for Oil B, recording only 93 and 60 h, respectively. On the other hand, Oil D, with a higher scuffing load-carrying capacity and micro-pitting ability, showed slightly lower pitting performance than Oil B, operating around 223 h without any pitting failures. Oil E, however, has shown the best performance even against pitting failure compared to both turbine oils and the automatic transmission fluid, with a time to pitting of around 251 h.

From the gear testing results, the ranking of the lubricants was made according to the specific gear failure modes, which showed evidence among the tested lubricating oils that Oil E (engine oil) has out-performed all the other oils in every single test conducted. Nevertheless, these standard test results were considered only as base line results for further evaluation of the lubricating oils using Brugger and SRV lab-scale tribometers under LOL experimental conditions.

### 3.4. Load-carrying capacity evaluated by Brugger tribometer

The Brugger experiment is suited to evaluate the load-carrying performance of the lubricants and its additives under boundary lubrication in short time (30 s) compared to other tribological methods. Although this is basically a quicker method, the contacts are depleting from lubricants over time in turn simulating the oil starvation condition but in a short period of time. The effect of lubricants and their additives to prevent the metal-metal contact is determined by the linear expanse of the contact area and the amount of wear on the cylindrical specimen as shown in Fig. 2. Since the boundaries of the wear scars are randomly formed, a non-contact confocal optical microscope is used to precisely determine the wear scar volume (see Fig. 9) and measure the diagonal lengths (a and b) of the elliptical wear scar as described in Fig. 2. The load-carrying capacities of the lubricating oils are calculated as defined in section 2 and using Eq. (1). The results show that Oil E (engine oil) has the highest load-carrying capacity and lowest wear, thus out-performing the other lubricating oils as recorded in Fig. 10 and Table 5. The lowest load-carrying capacity and high wear was observed for the Oil D (ATF) recording only half of the performance of Oil E corresponding to their viscosity levels (see Table 2). Despite having higher viscosity than Oils A, B and C, the performance of Oil D under starved lubrication is detrimental. Further, at oil starvation conditions, Oil D containing relatively low contents of phosphorus has failed severely, showing a wider and deeper wear scar than other lubricating oils as shown in Fig. 9. In contrast to that, high phosphorus containing turbine oils (Oil A and B) do not adequately improve the wear resistance and/or load-carrying capacities. However, Oil C with moderate and comparable amounts of phosphorus to Oil E has performed relatively better among turbine oils showing slightly improved load-carrying ability and wear

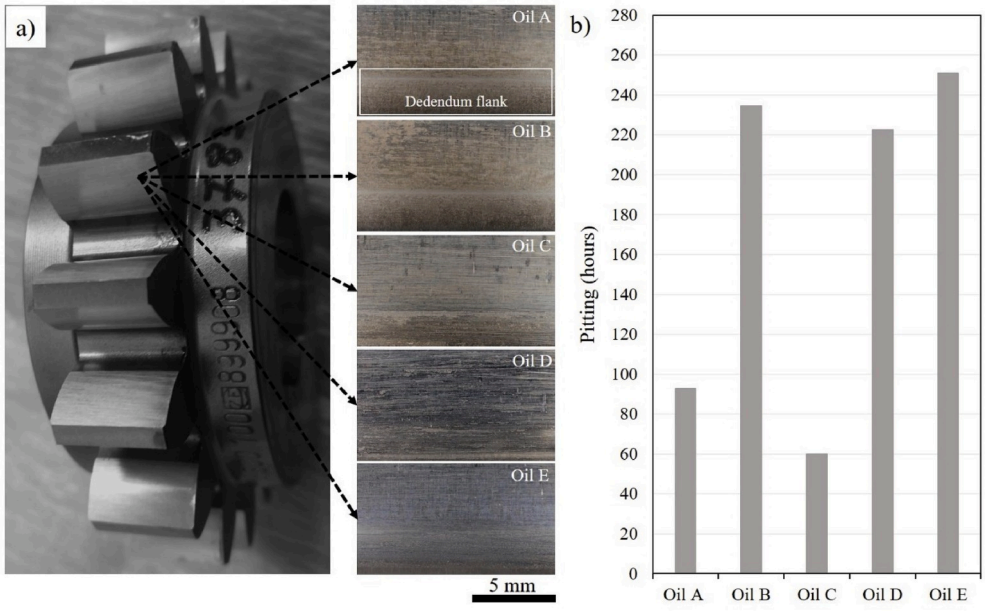


**Fig. 8.** a) Micro-pitting failures observed by light optical microscope on the flanks of the pinion spur gears tested using the FZG back-to-back gear test rig with the lubricating oils A to E and b) test hours until occurrence of pitting failure.

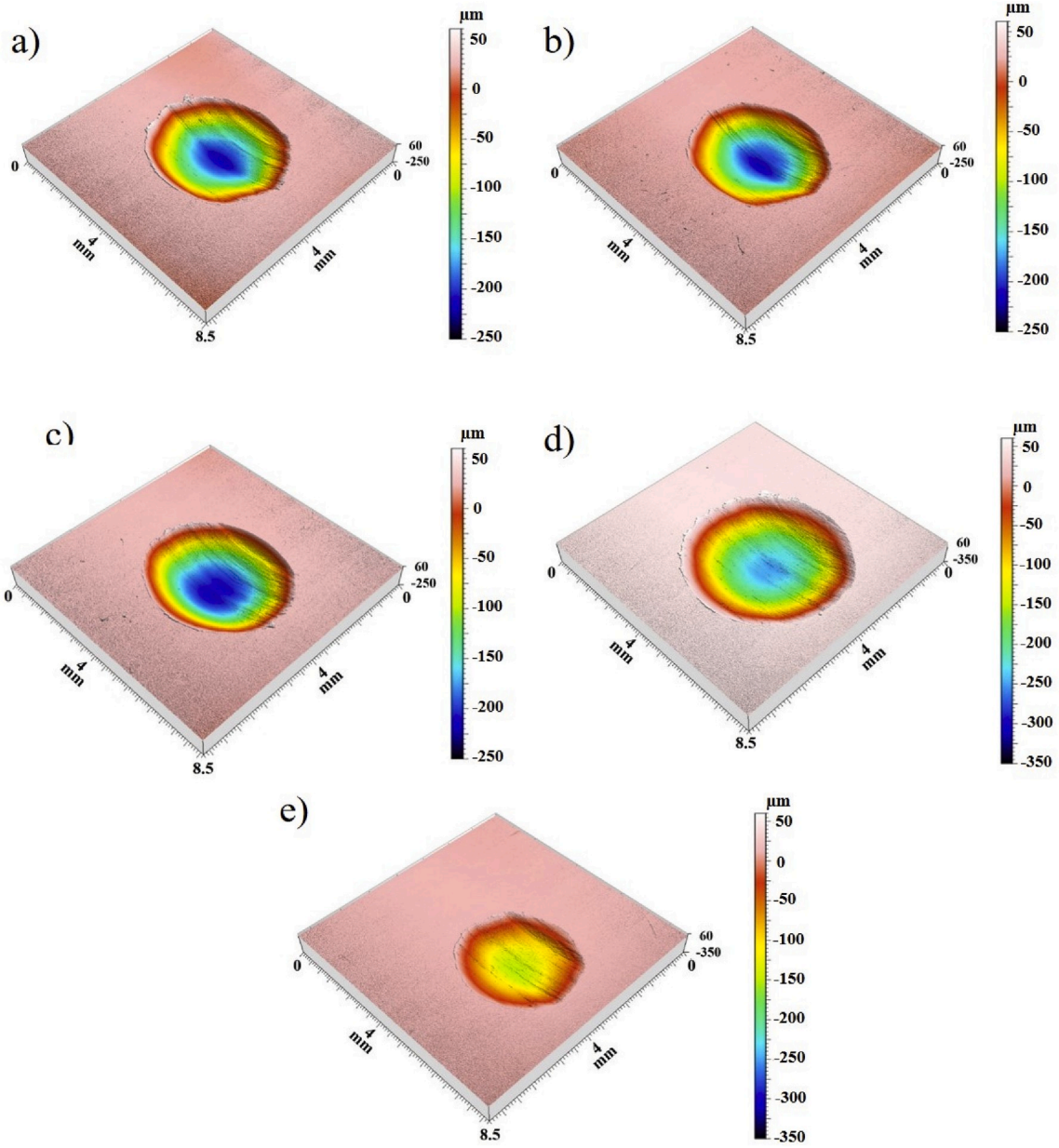


**Fig. 9.** 3D optical measurements by confocal microscopy of the elliptical wear scars on the cylindrical steel specimens tested using a) Oil A, b) Oil B, c) Oil C, d) Oil D and e) Oil E.

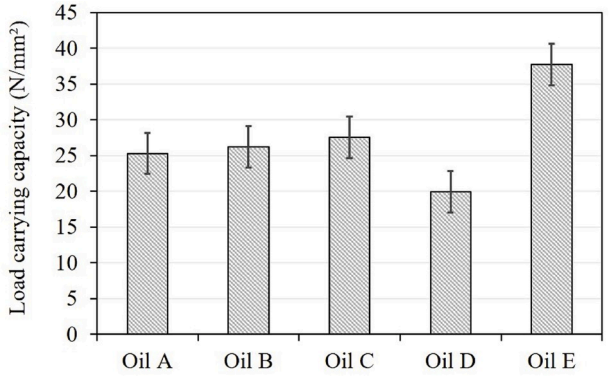


**Fig. 10.** Brugger test results showing the load-carrying capacity of the investigated oils.

**Table 5**
Wear depth and wear volumes produced on the cylindrical specimens by Brugger testing of the investigated oils.

| Lubricant Oils | Diagonal lengths (mm) | | Load Carrying Capacity (N/mm$^2$) | Wear depth (x10$^{-3}$ mm) | Wear volume (mm$^3$) |
|---|---|---|---|---|---|
| | a | b | | | |
| Oil A | 3.97 | 5.07 | 25.30 | 232 | 1.61 |
| Oil B | 3.96 | 4.95 | 26.24 | 224 | 1.64 |
| Oil C | 3.82 | 4.84 | 27.52 | 223 | 1.49 |
| Oil D | 4.55 | 5.61 | 19.95 | 305 | 2.88 |
| Oil E | 3.24 | 4.17 | 37.72 | 156 | 0.74 |

resistance. Besides, Oil E also contains high concentrations of other additive elements (sulfur, zinc, calcium) to survive extreme pressure and minimize abrasive wear in the contact. Thus, Brugger experiments revealed a correlation between the tribological results and the lubricant

chemistry, in particular wear protection additives.

### 3.5. Lubricant starvation evaluated by friction behavior using SRV tribometer

Three stages of frictional tests were conducted (see Fig. 11) and the tests were manually stopped once a sudden increase in friction associated with a relative increase in acoustic noise from the contact was realized. Only one out of 3 friction results from each oil has been shown to provide clear visibility and the average coefficient of friction values are shown in Fig. 12 for the running-in stage. The friction behavior of the lubricants shows no sudden changes in friction after running-in stage (shut-off of oil supply) indicating that the contact has some residual lubricant film and/or tribofilm formation. But a gradual increase in coefficient of friction is observed over time (especially for Oil C) until a sharp rise where the contacts starve without lubrication and induce scuffing. The friction level for the turbine oils (Oils A, B and C) were lower than Oil D and Oil E; the highest friction recorded was for Oil D (ATF) of about 0.13 during running in stage. After the running in stage, the coefficient of friction values gradually increased showing similar trends for Oil D and Oil E, but the lubricant film breaks much earlier for Oil D than Oil E. The less resistant nature of the oil film formed by Oil D is maybe due to a lower amount of phosphorus than other lubricating oils (see Table 2) for adequate contact protection.

As for the turbine oils, the following statements can be made: unlike Oils A and B, the degradation of the oil film for Oil C was visibly recorded after 6 min from the time of oil shut-off where an increase in coefficient of friction was observed from 0.09 to 0.12. Similar degradation of the tribofilm was also observed in the consecutive tests for Oil A and Oil B but always less pronounced than for Oil C. In Fig. 13, the time to failure is highlighted for the tested lubricants demonstrating no scuffing damage occurred in using Oil E throughout the test substantiating the LOL condition with prolonged lubrication time. SRV friction test tracks are further investigated using SEM, Raman spectroscopy and TEM to identify any possible tribofilm formation at the interface.

### 3.6. Surface characterization

#### 3.6.1. Scanning electron microscopy (SEM)

Further, the wear track from the friction test conducted with Oil D and Oil E have been analyzed using SEM-EDX. In case of Oil D, the wear track is scuffed severely leaving no traces of tribofilm at the contact zone (see Fig. 14). Fig. 15 shows the SEM image and corresponding EDX spectra at a random location on the wear track revealing the presence of additive elements in case of Oil E. This is verified in another random location on the wear track. The elements such as phosphorus, sulfur,

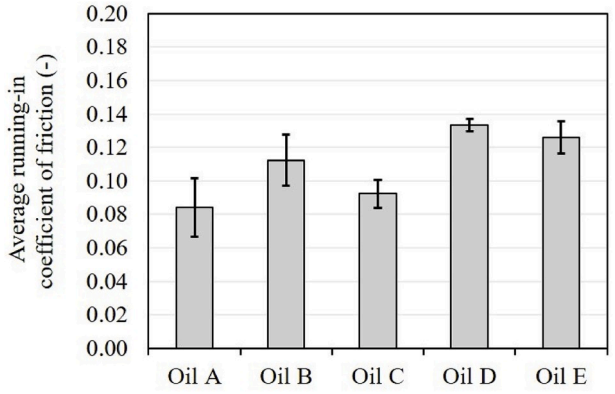


**Fig. 12.** Average coefficient of friction for running-in stage of the investigated oils.

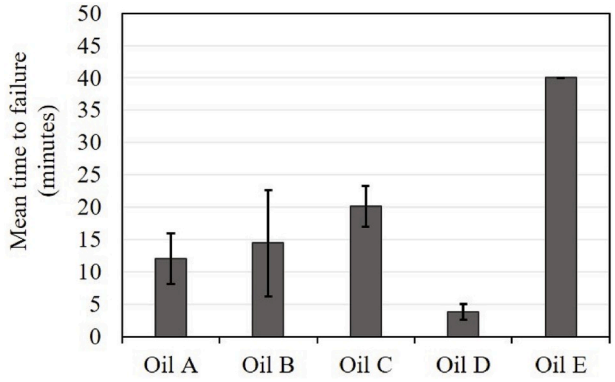


**Fig. 13.** Time to failure (time until scuffing initiation) after lubricant supply has been shut-off.

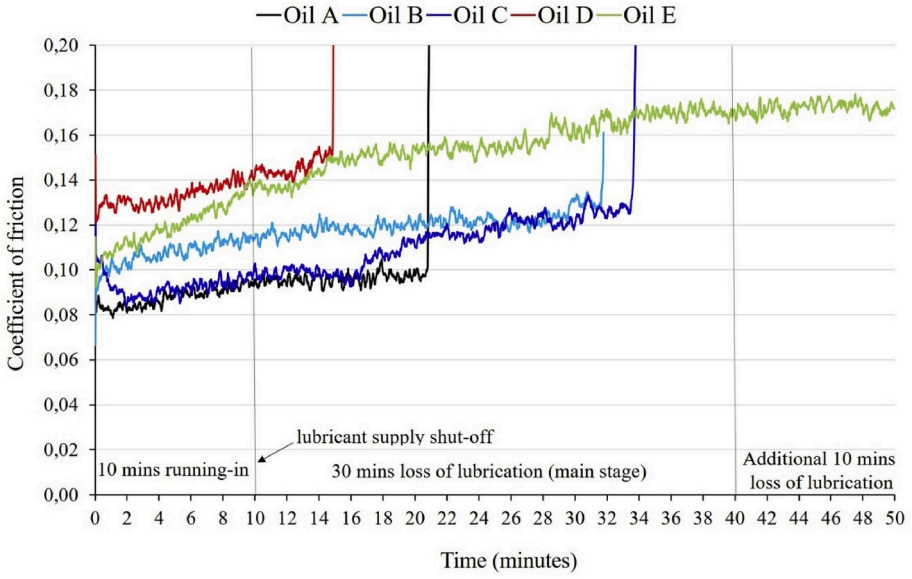


**Fig. 11.** Evolution of coefficient of friction from each oil (for better visibility only one friction curve for each lubricating oil has been shown and the statistics of all the experiments are presented in Fig. 12).

zinc, calcium and traces of silicon were observed in the wear track of Oil E confirming tribofilm formation. However, a significant change in the nature of tribofilm between the initial, start of LOL and in the end of the friction test is expected.

### 3.6.2. Raman spectroscopy

Additionally, the same sliding wear track from Oil E has been investigated using Raman spectroscopy (see Fig. 16) to confirm the type of chemical compounds present in the tribofilm. A relative strong peak was observed at the Raman peak of 950 $cm^{-1}$, which can be assigned to the vibration of P–O that is probably associated with zinc [45,46]. Furthermore, another peak at 1145 $cm^{-1}$ can be also assigned to P–O vibration, which indicates the existence of phosphates in the tribofilm [47]. At 660 $cm^{-1}$, a Raman peak of magnetite can be found as a typical reaction product for ferrous substrates after rubbing. The peak of $\gamma$-$Fe_2O_3$ at 725 $cm^{-1}$ is prominent due to a temperature-induced phase transformation [48]. Peaks related to $SO_4^{2-}$ are addressed at 418, 485, 618, and 1008 $cm^{-1}$ respectively. The peaks of $SO_4^{2-}$ can be attributed to the compounds of $ZnSO_4$ or $CaSO_4$ [49,50]. Finally, the peak at 330 $cm^{-1}$ is attributed to $FeS_2$ [51]. Several peaks observed in the recorded Raman spectra, corresponding to phosphate and sulfate, are attributed to different additive groups conforming the following types of binding: Fe-phosphate, Fe-sulfate, Zn-phosphate, Ca-phosphate and Ca-sulfate. The anti-wear protection in Oil E is given by a mixture of ZDDP and over based calcium and sulfate compounds.

### 3.6.3. Transmission electron microscopy (TEM)

TEM investigations are carried out for the well-performing lubricating oils (Oil C and E) under LOL condition in SRV (ball-on-disc) tribometer experiments. FIB slides from the SRV wear track were prepared by depositing a platinum protective layer on the area of interest. In Fig. 17, the separation of the platinum layer and the steel surface is clearly shown along with an insert displaying a closer view at the interface. A reference measurement was taken outside the wear track (Fig. 17 a) in order to differentiate between the regions with and without wear. The wear track from Oil C (Fig. 17 b) showed no traces of any tribofilm on the surface but a very thin layer of iron oxides demonstrating that the interface was clearly out of lubricant and exposed to the atmospheric oxygen. From Fig. 17 c, the formation of a tribofilm is evident for the friction test conducted using Oil E and it is only few nanometers (<10 nm) thick. However, the initial thickness of the film would have been much thicker because there was no lubrication medium after the running-in until the end of the experiment to further replenish the contact. This is in line with the findings from the corresponding Raman analysis showing the presence of traces of lubricating oil substances in the contact.

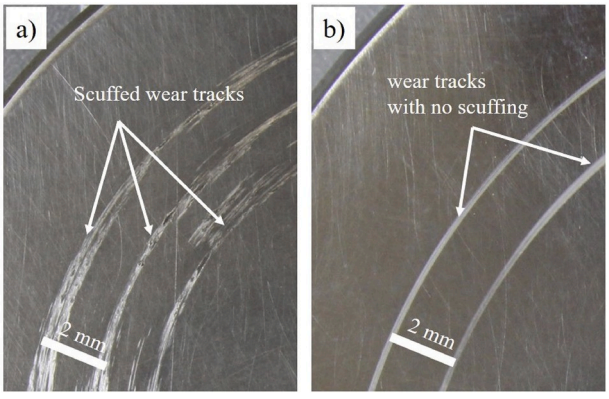


**Fig. 14.** Examples of wear tracks from sliding friction tests conducted for a) Oil D showing pronounced scuffing marks and b) Oil E without scuffing initiation.

## 4. Discussion

Gear tests under lubrication using FZG gear test rig show divergent results (see Figs. 4 and 5) for the chosen turbine oils regarding typical gear failure modes: scuffing, micro-pitting and pitting. Scuffing was greatly influenced by oil formulation, because one of the ester based synthetic turbine oils (Oil C, DOD-PRF-85734A) showed similar performance as the mineral based engine oil (Oil E, SAE 10W-40) although the oils were characterized by different anti-wear additive formulations, Oil C with TCP and Oil E with ZDDP and detergents. Despite other turbine oils (Oil A and B), the ester pattern of Oil C is well-structured and have higher boiling range (see Figs. 5 and 6). Oil D on the other hand, reached its scuffing limit with no further possibilities of improvement.

The oil performances against micro-pitting and pitting failures are considered as separate topics to be investigated as they invariably take longer time to test, unlike scuffing tests. At present, the findings from the micro-pitting results (e.g. grey regions) are comparable with the oil properties, because the grey regions are more pronounced for lower viscosity oils thereby reduced film thickness and significant asperity contacts, see Fig. 8a and Table 5. Micro-pitting failures occur due to mainly rolling-sliding surface contact fatigue, which is influenced by lubricant viscosity and surface roughness in other terms specific film thickness or lambda ratio [52–55]. Some research has found that the micro-pitting failures are influenced by the lubricant additives [56–59]. Pitting results on the other hand does correlate with the oil properties in general, except for Oil B, see Fig. 8b. This could be associated to the frictional characteristics of the oils tested using SRV tribometer, see Fig. 11. Having similar physical properties, the coefficient of friction is slightly higher for Oil B than oils A and C, relating to the different use of anti-wear additives, see Table 3. Consequently, further investigation is required involving changes in contact surface roughness and temperature that could certainly affect the properties of the tested lubricants and eventually micro-pitting and pitting failures. However, these results show an overview of long-term behavior of the tested lubricating oils. Nevertheless, the focus is mainly on the oil starvation conditions and the findings in this work will guide futureplanned activities in this research topic.

In contrast to the FZG standard lubrication test, Brugger and SRV tests were performed to allow the steel-steel contacts to operate initially with lubrication for a certain running-in time and later under oil starvation conditions. This is to determine the performance of additives working under boundary conditions such as anti-wear and extreme pressure additives. The load-carrying capacities from Brugger experiments for the turbine oils (Oil A, B, C) and ATF (Oil D) were 67%, 70%, 73% and 53% of that of engine oil (Oil E) and the time to scuffing failure from sliding (SRV) experiments were 30%, 36%, 50% and 10% of that of Oil E, respectively. In a tribological contact, the fluid film generating capability of a lubricant is quantified by the pressure-viscosity coefficient at a given temperature [60,61]. It is evident from the film thickness and lambda value from Table 4 that all the friction tests by SRV (ball-on-disc) were conducted under boundary lubrication, where the shear properties of the tribofilm becomes more significant. The protective layers on the sliding surfaces formed by chemical reaction with the lubricant tend to reduce the surface roughening and increase load-carrying capacity even when the $\lambda$ is as low as 0.03 [5]. On the other hand, a study conducted to determine the thickness of anti-wear films (ZDDP) using AFM technique showed a significant increase in the roughness of the film when compared with the initial surface roughness [62]. So, it is important to tailor the oil additive formulation to deliver smooth operations and to resist longer at the contact interface providing possible lubrication in the event of oil starvation conditions. This lambda value may explain the improved overall performance of Oil D in FZG gear tests under lubricated conditions (see Table 4) but is not suitable to operate in systems that are susceptible to oil starvation conditions where no recovery of the tribofilm takes place.

Overall, base oil viscosity is relevant in full lubrication in terms of

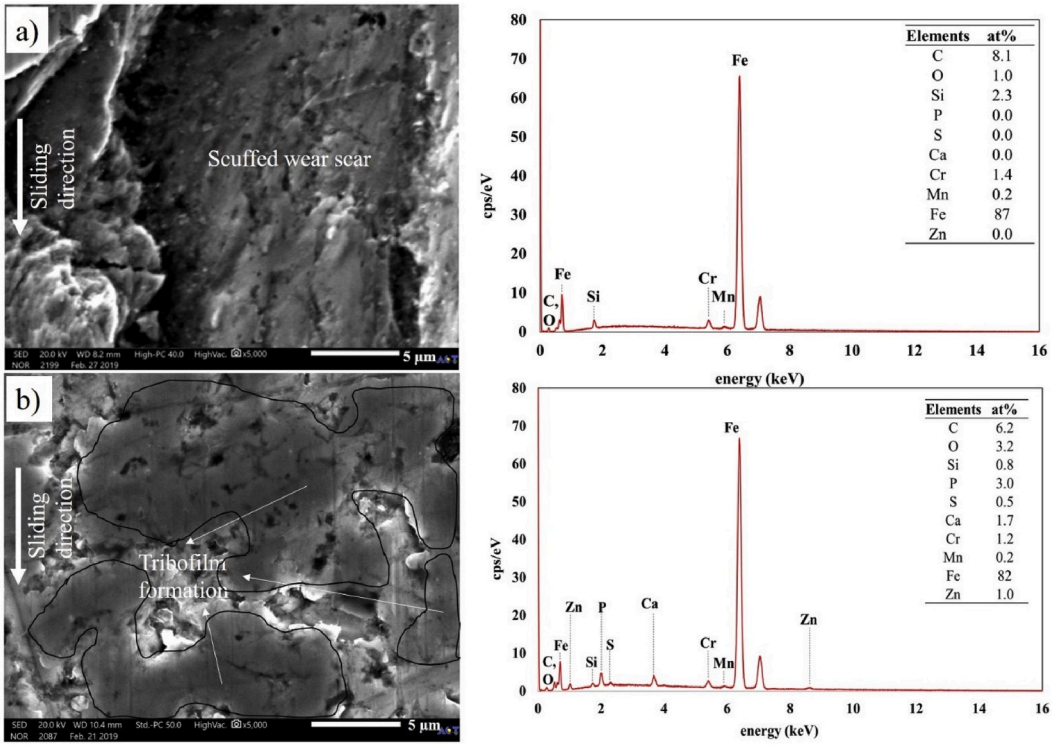


**Fig. 15.** SEM image and the corresponding EDX spectra taken at a random location on the friction test wear track of a) Oil D and b) Oil E.

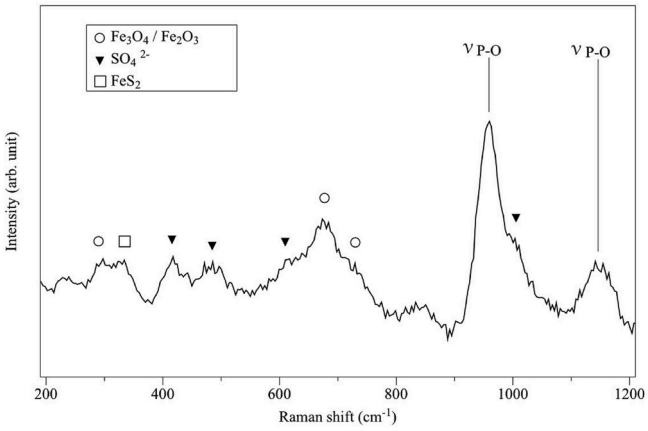


**Fig. 16.** Raman spectra analysis of the sliding friction test track formed by using Oil E.

load-carrying capacity of the lubricating oil whereas additive chemistry (anti-wear) is more relevant under oil starvation conditions in a gearbox.

The correlation between oil chemistry and the tribological evaluation can be conferred from Table 6. Base oil results from the GC-MS analysis revealed the detailed chemical structure of the base oil and wear protective additives used in each lubricant, which is one of the keys to determine the surface protection against scuffing. Base oil findings in this work explains the thermal stability (or volatility) of the synthetic ester oils over ester mixed PAO and mineral oils. Friction behavior under boundary lubrication regime could be explained by the type of wear protective additives identified in the oils. From the lubricating oil composition (see Table 6), significant amounts of phosphorus have been used commonly in all the tested lubricating oils, elucidating that phosphorus containing additive compounds are used widely to endure more stringent specifications such as in gearbox and engine applications. Turbine oils evaluated in this study contain mainly phosphate esters as their main additive element showing similar friction behavior for oils with only TCP additive but slightly higher friction for TCP combined with BuTPP additive (see Table 3 and Fig. 11). Since 1940s, TCP is known to reduce friction and wear under boundary lubrication conditions and BuTPP is developed as a substitute for TCP to minimize its volatility and toxicity [63]. Automatic transmission fluid (ATF) is formulated with only BuTPP and contains lower amounts of phosphorus. The lack of adequate concentration of phosphate anti-wear additives in lubricating oil may have severe impact on oil starvation conditions. In case of the engine oil, ZDDP has several functions comprising wear

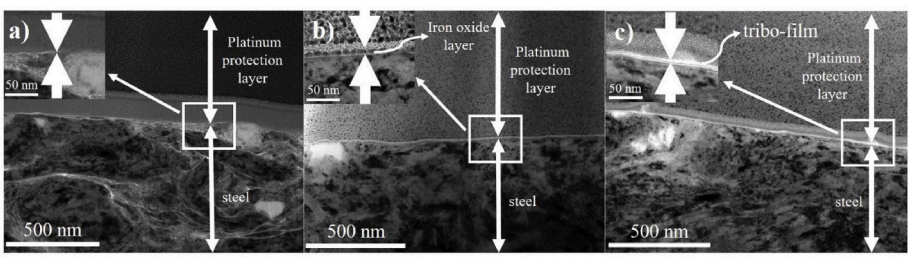


**Fig. 17.** High-resolution TEM image of a cross-section of a) reference surface (untested), b) the wear test track formed by using Oil C and c) the wear track formed by using Oil E.

**Table 6**
Correlation of results from lubricating oil composition and their performances under FZG back-to-back gear test rig, Brugger lubricant tester and SRV sliding tribometry experiments.

| | Lubricants | Oil A | Oil B | Oil C | Oil D | Oil E |
|---|---|---|---|---|---|---|
| Chemical composition (ppm) | Phosphorus (P) | 2400 | 2400 | 900 | 340 | 1000 |
| | Sulfur (S) | <10 | <10 | <10 | 800 | 4600 |
| | Zinc (Zn) | – | – | – | <10 | 1200 |
| | Calcium (Ca) | <5 | <5 | <5 | 50 | 3300 |
| | Silicon (Si) | <10 | <5 | <10 | <5 | <5 |
| FZG back-to-back gear test rig | Scuffing load level (−) | 10 | 9 | 12 ⬆ | 12 | 12 ⬆ |
| | Micropitting (−) | Medium resistance | Medium resistance | High resistance | High resistance | High resistance |
| | Pitting (hours) | 93 | 235 | 60 | 223 | 251 |
| Brugger lubricant tester | Load-carrying capacity ($N/mm^2$) | 25.3 | 26.2 | 27.5 | 20.0 | 37.7 |
| | Wear volume ($mm^3$) | 1.61 | 1.64 | 1.49 | 2.88 | 0.74 |
| SRV sliding test | Average running-in coefficient of friction (−) | 0.08 | 0.11 | 0.09 | 0.13 | 0.13 |
| | Mean time to failure (minutes) | 12.0 | 14.4 | 20.1 | 3.83 | 40.0 |

protection and prevention of oxidation as well as corrosion inhibition. Additionally, phosphorus and sulfur react with steel surface forming iron phosphate and iron sulfide (and sulfate) compounds that can reduce surface wear by preventing direct metal contacts [22]. Calcium containing additive compounds such as calcium sulfonate, calcium carbonate and calcium phosphate in engine oil can influence the boundary films formed by ZDDP contributing to additional wear protection [22]. Surface analysis by SEM-EDX and Raman spectra on the wear tracks produced by SRV (ball-on-disc) sliding experiment using Oil E reveals that the engine oil generates a tribofilm during running-in providing enhanced residual lubrication that persists longer under LOL conditions. Although, engine oil showed the best results in every single LOL experiment conducted, the friction behavior is elevated, and the volatility is significantly higher than that of turbine oils. Moreover, the nature of the tribofilm formation depends on the test conditions (pure sliding) used in this work, therefore the oils could perform differently if they are subjected to both sliding and rolling contact conditions.

From experimental findings in this work, a ranking of the tested lubricating oils based on the scuffing performance from both the gear tests and the lab scale tests can be given as:

| | Lubricated condition (FZG gear testing) | Loss of lubrication condition (Lab-scale pure sliding contacts) |
|---|---|---|
| Good | Oil C and E | Oil E |
| Moderate | Oil D | Oil A, B and C |
| Not recommended | Oil A and B | Oil D |

## 5. Conclusions

Loss of lubrication (LOL) in rotorcraft transmissions is one of the major safety concerns in helicopter industry. In this work, three ester-based synthetic lubricating oils, one ester mixed PAO synthetic lubricating oil and one mineral-based lubricating oil are investigated. Complementary to other research articles on LOL, this work aimed to provide a comprehensive investigation on the lubricating oil chemistry. The influence of oil formulation was demonstrated both under lubrication and LOL conditions. Based on this experimental work, the following conclusions can be drawn:

- Lubricating oil analysis by GC-MS provides an in-depth knowledge about the structure of the base oil and the type of additives used in the oils, which supported all the tribological investigations in this work. The initial boiling point for the synthetic ester base oils are higher than that of ester mixed PAO and mineral oil, thereby, indicating lower volatility with increase in temperature.
- The standard lubrication tests by FZG gear test rig provide reliable results on the typical gear failure modes: scuffing, micro-pitting and pitting. Scuffing performance between a well-structured synthetic ester base oil (Oil C) and a mineral base oil (Oil E) is similar irrespective of their viscosity range and the type of wear protection additive used in each oil.
- FZG gear test rigs are not feasible to study the performance behavior of the lubricating oils under LOL conditions and the full-scale experiments often generate high costs, so lab-scale Brugger (cylinder-on-ring) and SRV (ball-on-disc) tribotests, simulating a single point contact condition of gear mesh, are implemented.
- LOL tests exclude the viscosity effects after a certain running-in time and the wear protection until scuffing is totally attributed to the anti-wear additives used in the respective oil. Synthetic ester oils formulated with aryl phosphate (TCP) additives show lower friction coefficients than of the other oils tested. Although, ester mixed PAO oil contains aryl phosphate (BuTTP) based additive, its friction behavior is similar to that of the mineral oil with ZDDP. Conversely, the base oil selection for LOL performance is also very important as the ester oils sustained the starvation condition longer than ester mixed PAO oils.
- Both TCP and ZDDP anti-wear additives provide scuffing resistance under LOL condition, however, Calcium and Sulfur based compounds tend to have constructive effect by co-adsorbing in the tribofilm which could also be a choice for LOL conditions provided the contact is adequately lubricated during the running-in process.

Nevertheless, several other factors such as alternative (high temperature) materials, super finished surfaces, surface textures and coatings must be evaluated under LOL conditions to support a better lubricant formulation for the rotorcraft transmission application. Moreover, tribometrical experiments simulating gear contact conditions with rolling-sliding motion could provide additional data on the investigated lubricating oils in terms of tribofilm formation and scuffing initiation, which will be studied in the future research work. Eventually, the impact of oil degradation upon lubrication and LOL deserves attention to verify whether the demand for operability is ensured once LOL occurs in the rotorcraft transmission. The findings in this work are considered to support future work in offering an oil formulation being more suitable for operation in the event of LOL.

## Declaration of competing interest

The authors declare that they have no known competing financial interests or personal relationships that could have appeared to influence the work reported in this paper.

## CRediT authorship contribution statement

**Azhaarudeen Anifa Mohamed Faruck:** Investigation, Writing - review & editing, Validation. **Chia-Jui Hsu:** Writing - review & editing. **Nicole Doerr:** Investigation, Writing - review & editing, Supervision. **Michael Weigand:** Writing - review & editing, Supervision. **Carsten Gachot:** Conceptualization, Writing - review & editing, Supervision, Validation.

## Acknowledgements

The research work was funded by the Austrian COMET program (K2 projects XTribology, no. 849109, and InTribology, no. 872176) and the Endowed Professorship on "Tribology" at the Vienna University of Technology (grant no. WST3-F-5031370/001-2017). The work was jointly carried out at the "Excellence Centre of Tribology" (AC2T research GmbH) and the Vienna University of Technology. Authors would like to thank Dr. Andjelka Ristic, Mr. Michael Schandl and all the co-workers who assisted in obtaining lubricant and surface analysis at AC2T research GmbH, Wiener Neustadt, Austria, and Dr. Johannes Bernardi and Mr. Andreas Steiger-Thirsfeld for their support in TEM measurements at TU Wien.

## References

[1] Transportation Safety Board of Canada. Main gearbox malfunction/collision with water, aviation investigation report (A09A0016). In: St. Johns's, newfoundland and labrador. Transportation Safety Board of Canada; 2009.
[2] European Aviation Safety Agency. Certification specifications for large rotorcraft CS-29 (amendment 3). EASA-CS-29; 2012.
[3] Ads-50-PRF. Aeronautical design standard: rotorcraft propulsion performance and qualification requirements and guidelines. ST.Louis, Missouri: United States Army Aviation Troop Comand; 1996.
[4] Bowman WF, Stachowiak GW. A review of scuffing models. Tribol Lett 1996: 113–31. https://doi.org/10.1007/BF00160970.
[5] Lee YZ, Ludema KC. The effects of surface roughening and protective film formation on scuff initiation in boundary lubrication. 1991. https://doi.org/10.1115/1.2920619.
[6] Ludema KC. A review of scuffing and running-in of lubricated surfaces, with asperities and oxides in perspective. Wear 1984:315–31. https://doi.org/10.1016/0043-1648(84)90019-X.
[7] Wojciechowski M Wieczorowski, Mathia TG. Transition from the boundary lubrication to scuffing – the role of metallic surfaces morphology. Wear 2016: 39–49. https://doi.org/10.1016/j.wear.2017.09.011.
[8] Davis JR. Gear Tribology and lubrication, gear materials, properties, and manufacture. Materials Park, OH.: ASM International; 2005.
[9] Semenov AP. The phenomenon of seizure and its investigation. Wear 1961:1–9. https://doi.org/10.1016/0043-1648(61)90236-8.
[10] Matveevsky RM. Friction power as a criterion of seizure with sliding lubricated contact. Wear 1992:1–5. https://doi.org/10.1016/0043-1648(92)90103-F.
[11] Drozdov YN. Thermal aspects of scoring in simultaneous rolling and sliding contact. Wear 1972:201–9. https://doi.org/10.1016/0043-1648(72)90382-1.
[12] Lee SC, Chen H. Experimental validation of critical temperature-pressure theory of scuffing. Tribol Trans 1995:738–42. https://doi.org/10.1080/10402009508983467.
[13] Blok H. Measurement of temperature flashes on gear teeth under extreme pressure conditions. Proc Inst Mech Eng 1937:14–20.
[14] Batchelor AW, Stachowiak GW. Some kinetic aspects of extreme pressure lubrication. Wear 1986:185–99. https://doi.org/10.1016/0043-1648(86)90096-7.
[15] Spikes HA, Cameron A. "Scuffing as a desorption process—an explanation of the borsoff effect. ASLE Trans 1974:92–6. https://doi.org/10.1080/05698197408981442.
[16] Wojciechowski Ł, Mathia TG. The polarity of metallic surfaces in the context of the corrosive and scuffing wear control. Tribol Int 2015:473–80. https://doi.org/10.1016/j.triboint.2015.05.012.
[17] Wojciechowski Ł, Mathia TG. Conjecture and paradigm on limits of boundary lubrication. Tribol Int 2015;(82):577–85. https://doi.org/10.1016/j.triboint.2014.02.006.
[18] Dawson PH. Effect of metallic contact on the pitting of lubricated rolling surfaces. J Mech Eng Sci 1962;(4):16–21. https://doi.org/10.1243/jmes_jour_1962_004_005_02.
[19] Anderson W, Carter T. Effect of lubricant viscosity and type on ball fatigue life. Wear 1959. https://doi.org/10.1016/0043-1648(59)90176-0.
[20] Davidson TF, Ku PM. The effect of lubricants on gear tooth surface fatigue. ASLE Trans 1958:40–50. https://doi.org/10.1080/05698195808972313.
[21] Martin JM, Grossiord C, Le Mogne T, Igarashi J. Transfer films and friction under boundary lubrication. Wear 2000;(245):107–15. https://doi.org/10.1016/S0043-1648(00)00471-3.
[22] Martin JM. Antiwear mechanisms of zinc dithiophosphate: a chemical hardness approach. Tribol Lett 1999;(6):1–8. https://doi.org/10.1023/A:1019191019134.
[23] Martin JM, Onodera T, Minfray C, Dassenoy F, Miyamoto A. The origin of anti-wear chemistry of ZDDP. Faraday Discuss 2012;(156):311–23. https://doi.org/10.1039/c2fd00126h.
[24] Johnson DW, Bachus M, Hils JE. Interaction between lubricants containing phosphate ester additives and stainless steels. Lubricants 2013:48–60. https://doi.org/10.3390/lubricants1020048.
[25] Townsend DP, Coy JJ, Hatvani BR. OH-58 helicopter transmission failure analaysis. NASA; 1992.
[26] Michaelis K, Hoehn BR, Oster P. Influence of lubricant on gear failures - test methods and application to gearboxes in practice. Tribotest 2004;(11):43–56. https://doi.org/10.1002/tt.3020110105.
[27] Paton CG, Maciejewski WB, Melley RE. Test methods for open gear lubricants. Lubr Eng 1990;(46):318–26.
[28] Coe HH. Thermal analysis of a planetary transmission with spherical roller bearings operating after complete loss of oil. NASA Tech. Pap.; 1984.
[29] Handschuh RF. Lubrication system failure baseline gear mesh testing on an aerospace quality. Wilfredo Morales - Natl. Aeronaut. Sp. Adm.; 2000.
[30] Gasparini G, Motta N, Gabrielli A, Colombo D. Gearbox loss of lubrication performance: myth, art or science? 40th Eur. Rotorcr. Forum 2014;(2):1162–75.
[31] Riggs MR, Murthy NK, Berkebile SP. Scuffing resistance and starved lubrication behavior in helicopter gear contacts: dependence on material, surface finish, and novel lubricants. Tribol Trans 2017:932–41. https://doi.org/10.1080/10402004.2016.1231358. 60.
[32] Fenske G, Ajayi O, Erck R, Lorenzo-Martin C, Masoner A, Comfort A. Reliability of powertrain components exposed to extreme tribological environments. In: Proceedings of the 2010 ground vehicle systems engineering and Technology symposium; 2010. Michigan.
[33] Podgornik B, Vižintin J, Jacobson S, Hogmark S. Tribological behaviour of WC/C coatings operating under different lubrication regimes. Surf Coating Technol 2004: 558–65. https://doi.org/10.1016/S0257-8972(03)00927-7. 177-178.
[34] Eichler JW, Matthews A, Leyland A, Doll GL. The influence of coatings on the oil-out performance of rolling bearings. Surf Coating Technol 2007:1073–7. https://doi.org/10.1016/j.surfcoat.2007.07.048. 202.
[35] ASTM D7042. Test method for dynamic viscosity and density of liquids by stabinger viscometer (and the calculation of kinematic viscosity). American National Standard Institute; 2013. https://doi.org/10.1520/D7042-12A.2.
[36] ASTM D2270. Standard practice for calculating viscosity index from kinematic viscosity at 40 °C and 100 °C. ASTM Int.; 2016. https://doi.org/10.1520/C0305-06.2.
[37] ASTM-D6352. Standard test method for boiling range distribution of petroleum distillates in boiling range from 174 °C to 700 °C by gas chromatography. Conshohocken, PA, USA: ASTM Int. West; 2019.
[38] Besser C, et al. Generation of engine oils with defined degree of degradation by means of a large scale artificial alteration method. Tribol Int 2019;(132):39–49. https://doi.org/10.1016/j.triboint.2018.12.003.
[39] Dörr N, Agocs A, Besser C, Ristić A, Frauscher M. Engine oils in the field: a comprehensive chemical assessment of engine oil degradation in a passenger car. Tribol Lett 2019. https://doi.org/10.1007/s11249-019-1182-7.
[40] Dörr N, et al. Correlation between engine oil degradation, tribochemistry, and tribological behavior with focus on ZDDP deterioration. Tribol Lett 2019. https://doi.org/10.1007/s11249-019-1176-5.
[41] DIN ISO 14635-1. FZG-Prüfverfahren A/8,3/90 zur Bestimmung der Fresstragfähigkeit von Schmierölen. 2006. Test.
[42] Deutsches Institut Fur Normung EV. Din 51347: testing of lubricants - testing under boundary lubricating conditions with the Brugger lubricant tester - Part 1 and Part 2: procedure for lubricating oils. Berlin, Ger.: Dtsch. Inst. für Normung; 2000.
[43] Wu CS, Klaus EE, Duda JL. Development of a method for the prediction of pressure-viscosity coefficients of lubricating oils based on free-volume theory. Baltimore, Md: Presented at the ASME/ASLE Joint Tribology Conference; 1988. p. 121–8. 111.
[44] Hamrock BJ, Dowson D. Isothermal elastohydrodynamic lubrication of point contacts: Part III-fully flooded result. J Tribol 1977;(99):264–75. https://doi.org/10.1115/1.3453074.
[45] Gauvin M, Dassenoy F, Minfray C, Martin JM, Montagnac G, Reynard B. Zinc phosphate chain length study under high hydrostatic pressure by Raman spectroscopy. J Appl Phys 2007. https://doi.org/10.1063/1.2710431.
[46] Berkani S, et al. Structural changes in tribo-stressed zinc polyphosphates. Tribol Lett 2013;(51):489–98. https://doi.org/10.1007/s11249-013-0188-9.
[47] Pemberton JE, Latifzadeh L, Fletcher JP, Risbud SH. Raman spectroscopy of calcium phosphate glasses with varying CaO modifier concentrations. Chem Mater 1991;(3):195–200. https://doi.org/10.1021/cm00013a039.
[48] de Faria DLA, Venâncio Silva S, de Oliveira MT. Raman microspectroscopy of some iron oxides and oxyhydroxides. J Raman Spectrosc 1997;(28):873–8. https://doi.org/10.1002/(sici)1097-4555(199711)28:11<873::aid-jrs177>3.3.co;2-2.
[49] Liu Y, Wang A, Freemen JJ. Raman, MIR, and NIR spectroscopic study of calcium sulfates: gypsum, bassanite, and anhydrite. Lunar Planet. Sci. Conf. 2009. https://doi.org/10.1063/1.3233935.
[50] Falgayrac G, Sobanska S, Brémard C. Raman diagnostic of the reactivity between ZnSO4 and CaCO3 particles in humid air relevant to heterogeneous zinc chemistry in atmosphere. Atmos Environ 2014;(85):83–91. https://doi.org/10.1016/j.atmosenv.2013.11.073.
[51] Gachot C, et al. Microstructural and chemical characterization of the tribolayer formation in highly loaded cylindrical roller thrust bearings. Lubricants 2016. https://doi.org/10.3390/lubricants4020019.

[52] Liu JY, Tallian TE, McCool JI. Dependence of bearing fatigue life on film thickness to surface roughness ratio. A S L E Trans.; 1975. p. 144–52. https://doi.org/10.1080/05698197508982757. 18.
[53] Townsend DP, Shimski J. Evaluation of the EHL film thickness and extreme pressure additives on gear surface fatigue life. NASA Tech. Memo.; 1994.
[54] Rycerz P, Kadiric A. The influence of slide–roll ratio on the extent of micropitting damage in rolling–sliding contacts pertinent to gear applications. Tribol Lett 2019. https://doi.org/10.1007/s11249-019-1174-7.
[55] Krantz TL. On the correlation of specific film thickness and gear pitting life, American Gear Manufacturer Association. Fall Tech. Meet. 2014:1–26. NASA/TM—2015-218711.
[56] Cardoso NFR, Martins RC, Seabra JHO, Igartua A, Rodríguez JC, Luther R. Micropitting performance of nitrided steel gears lubricated with mineral and ester oils. Tribol Int 2009;(42):77–87. https://doi.org/10.1016/j.triboint.2008.05.010.
[57] Benyajati C, Olver AV, Hamer CJ. An experimental study of micropitting, using a new miniature test-rig. Tribol 2003;(43):601–10. https://doi.org/10.1016/s0167-8922(03)80088-3.
[58] Lainé E, Olver AV, Beveridge TA. Effect of lubricants on micropitting and wear. Tribol Int 2008;(41):1049–55. https://doi.org/10.1016/j.triboint.2008.03.016.
[59] Lainé E, Olver AV, Lekstrom MF, Shollock BA, Beveridge TA, Hua DY. The effect of a friction modifier additive on micropitting. Tribol Trans 2009;(52):526–33. https://doi.org/10.1080/10402000902745507.
[60] Errichello R. Selecting oils with high pressure - viscosity coefficient - increase bearing life by more than four times. 2004. Machinery Lubrication.
[61] Larsson R, Kassfeldt E, Byheden Å, Norrby T. Base fluid parameters for elastohydrodynamic lubrication and friction calculations and their influence on lubrication capability. J Synth Lubric 2001;(18):183–98. https://doi.org/10.1002/jsl.3000180302.
[62] Topolovec-Miklozic K, Forbus TR, Spikes HA. Film thickness and roughness of ZDDP antiwear films. Tribol Lett 2007;(26):161–71. https://doi.org/10.1007/s11249-006-9189-2.
[63] On the mechanism of boundary lubrication. II. Wear prevention by addition agents. Proc. R. Soc. London. Ser. A. Math. Phys. Sci. 1940:103–18. https://doi.org/10.1098/rspa.1940.0113. 177.